Pavement Responses due to Static Rectangular Loadings using Classical Transform Integrals

J. W. Maina
CSIR Built Environment, Pretoria, South Africa

K. Matsui
Department of Civil and Environmental Engineering, Tokyo Denki University, Saitama, Japan

ABSTRACT: In recent years, there has been a worldwide shift in pavement design from empirical to mechanistic-empirically based methods. With this trend, a need for numerical analysis tools with the ability to simulate loading shape that closely resembles footprint of a tire acting on the pavement surface has started to emerge. With its Stress-in-Motion (SIM) technology, South Africa is well placed to lead this effort where three-dimensional tire-pavement contact stresses and tire foot-prints can be used to calibrate rectangular loading models for use in numerical analysis. The objective of this paper is to present closed-form solutions of pavement responses due to static rectangular loadings as a special case to wave propagation problems. In this study, two classical mathematical methods i.e. classical transform integral and classical potential function methods were investigated for flexibility and efficiency. The former was adopted in this study and a formulation of pavement responses is presented in this paper. This method is flexible and may easily be extended to dynamic and wave propagation analyses. Results of the new approach are validated by comparing its results with results obtained using GAMES software (for same load magnitude and loaded area) that is widely used in Japan and South Africa for axi-symmetric analysis of pavement structure.

KEY WORDS: Pavement, rectangular load, static analysis.

1 GENERAL INTRODUCTION

By supporting movement of people and goods, a sound road network plays a key role in socio-economic development of a country. In order to better understand impact of the increased loading on roads, studies on tire-road interaction have gained prominence in recent years. Tires form an essential interface between vehicles and road pavement surfaces. These are the only parts of the vehicle that are in contact with the road and transmit the vehicle loading to the road surface through a very small contact area, generally called the ‘contact patch’ or ‘tire foot-print’. By using fewer tires and carrying heavier cargo, modern trucks are exerting much higher contact stresses on the road surface than their predecessors. A good understanding of tire-road contact stresses is, therefore, important for better road pavement designs, and, hence, improved performance. A technique referred to as Stress-In-Motion (SIM), which may be seen as a next generation of the well known Weigh-In-Motion (WIM) axle/truck weigh technologies, has been developed with specific use in capturing individual tyre loads and 3D contact stresses for the sole purpose of improved mechanistic-empirical road pavement design and analysis (De Beer, 2008, Morgan et. al, 2007). This technique has

shown that tire-pavement contact stresses to be mostly rectangular and not circular in shape.

Cartesian coordinate system may be convenient in dealing with the uniform/non-uniform load acting over rectangular area, but there are few research reports on the derivation of its theoretical solution. Bufler (1971) derived the theoretical solution for multilayered systems using Cartesian coordinate system but did not provide any worked example. Further, Ernian (1989) used both cylindrical and Cartesian coordinate systems to derive solutions for both circular and rectangular uniformly distributed loads acting on the surface of a multilayered system. The approach presented by Ernian is very resourceful but still complicated because it involves considerable algebra.

2 THREE DIMENSIONAL PROBLEM OF ELASTICITY THEORY

There are mainly three methods that may be used to solve problems of the theory of elasticity (Borodachev, 1995, 2001). In the first one, the displacement vector is determined first, and this vector is then used to determine the stress and strain tensors (problem in displacements). Next, there is a second method where the stress tensor is determined first, and then this tensor is used to determine the strain tensor and displacement vector (problem in stresses). Lastly, in the third method the strain tensor is determined first, and then stress and displacement tensors are determined (problem in strains). The work presented in this paper deals with the first method of problem in displacements.

In this regard and for 3D problems, the Navier equations are the most convenient representation for the field equations. However, they are cumbersome to deal with because of the need to solve three coupled partial differential equations for the three displacement components. The difficulty with finding particular solutions of the system of equations in terms of the displacements arises because each of the sought deflection functions in Cartesian coordinates (x, y, and z) appear in all three equilibrium equations.

However, the solution may be simplified by representing displacements in terms of harmonic potentials. It is because this approach decouples the equations and there are various ways to do this. The most common approach is to use the so called Papkovich-Neuber potentials to represent the solution (Ozawa *et al.* 2009, Borodachev and Astanin, 2008). This enables one to use a well-known catalogue of particular solutions of the Laplace equation and sometimes even reduce the problem if not completely to one of the classical problems of the theory of harmonic functions (theory of potential). Despite the simplification, it is difficult to extend this approach to problems of dynamic or moving load analysis (Ozawa, *et al.* 2010).

The objective of this paper, therefore, is to present closed-form solution of pavement responses due to static rectangular loadings as a special case to wave propagation problems. In this study, a more flexible and efficient classical transform integral method is utilized as opposed to classical potential function method based on Papkovich-Neuber potentials.

3 GENERAL THEORY

A system of rectangular Cartesian coordinates (x, y, z) is used. By assuming the body forces to be zero, equilibrium equations may be written as:

$$\frac{\partial \sigma_x}{\partial x} + \frac{\partial \tau_{xy}}{\partial y} + \frac{\partial \tau_{xz}}{\partial z} = 0 \tag{1a}$$

$$\frac{\partial \tau_{xy}}{\partial x} + \frac{\partial \sigma_y}{\partial y} + \frac{\partial \tau_{zy}}{\partial z} = 0 \tag{1b}$$

$$\frac{\partial \tau_{xz}}{\partial x} + \frac{\partial \tau_{yz}}{\partial y} + \frac{\partial \sigma_z}{\partial z} = 0 \tag{1c}$$

where σ_x, σ_y, σ_z, τ_{xy}, τ_{xz}, and τ_{yz} are stresses in an infinitesimal element. Strain-displacement relationship may be represented as follows:

$$\varepsilon_x = \frac{\partial u}{\partial x},\ \varepsilon_y = \frac{\partial v}{\partial y},\ \varepsilon_z = \frac{\partial w}{\partial z},\ \gamma_{xy} = \frac{\partial v}{\partial x} + \frac{\partial u}{\partial y},\ \gamma_{xz} = \frac{\partial u}{\partial z} + \frac{\partial w}{\partial x},\ \gamma_{yz} = \frac{\partial w}{\partial y} + \frac{\partial v}{\partial z} \tag{2}$$

where u, v, and w are displacements in the directions of x-, y-, and z-axes. Furthermore, ε_x, ε_y, and ε_z are normal strains corresponding to normal stresses σ_x, σ_y, and σ_z, while γ_{xy}, γ_{xz}, and γ_{yz} are shear strains corresponding to shear stresses τ_{xy}, τ_{xz}, and τ_{yz}. Boundary conditions for rectangular loads acting on a surface of a semi-infinite medium shown in Figure 1 may be represented as shown below:

when $x \le |a|$ and $y \le |b|$ then;

$$\sigma_z(x, y, 0) = -p_z,\quad \tau_{xz}(x, y, 0) = -p_x,\quad \tau_{yz}(x, y, 0) = -p_y \tag{3a}$$

when $x > |a|$ and $y > |b|$ then;

$$\sigma_z(x, y, 0) = \tau_{xz}(x, y, 0) = \tau_{yz}(x, y, 0) = 0 \tag{3b}$$

Using Lame's constants, stress-strain relationship may be written as:

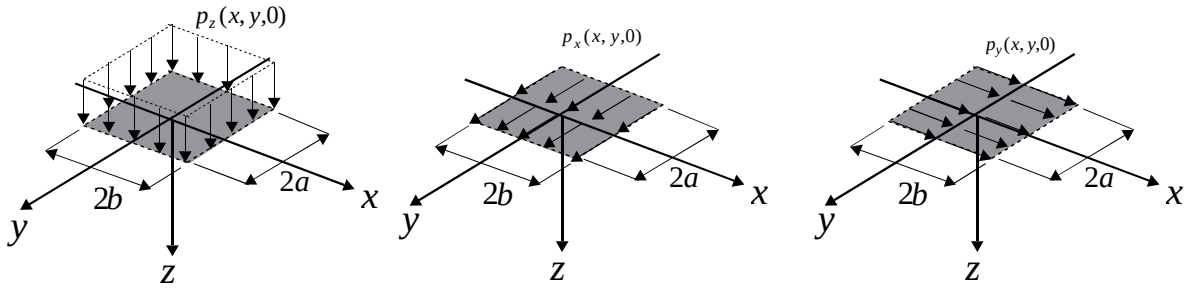

(a) vertical $p_z(x, y, 0)$ (b) horizontal $p_x(x, y, 0)$ (c) horizontal $p_y(x, y, 0)$

Figure 1: Uniformly distributed rectangular loads

$$\begin{Bmatrix}\sigma_x\\ \sigma_y\\ \sigma_z\\ \tau_{xy}\\ \tau_{xz}\\ \tau_{yz}\end{Bmatrix}=\begin{pmatrix}\lambda+2\mu & \lambda & \lambda & 0 & 0 & 0\\ \lambda & \lambda+2\mu & \lambda & 0 & 0 & 0\\ \lambda & \lambda & \lambda+2\mu & 0 & 0 & 0\\ 0 & 0 & 0 & \mu & 0 & 0\\ 0 & 0 & 0 & 0 & \mu & 0\\ 0 & 0 & 0 & 0 & 0 & \mu\end{pmatrix}\begin{Bmatrix}\varepsilon_x\\ \varepsilon_y\\ \varepsilon_z\\ \gamma_{xy}\\ \gamma_{xz}\\ \gamma_{yz}\end{Bmatrix} \tag{4}$$

where

$$\lambda=\frac{E\nu}{(1+\nu)(1-2\nu)},\quad \mu=\frac{E}{2(1+\nu)} \tag{5}$$

E is elastic modulus and ν is Poisson's ratio. Since in a multilayered system, layer materials and thicknesses may be different, Eqs (1), (2), and (4) have to be derived for each layer. Substituting Eqs (2) and (4) into Eq (1), Navier's equations may, in the absence of body forces, be obtained as functions of displacements as shown below:

$$(\lambda+2\mu)\frac{\partial^2 u}{\partial x^2}+\mu\frac{\partial^2 u}{\partial y^2}+\mu\frac{\partial^2 u}{\partial z^2}+(\lambda+\mu)\frac{\partial^2 v}{\partial x\,\partial y}+(\lambda+\mu)\frac{\partial^2 w}{\partial x\,\partial z}=0 \tag{6a}$$

$$(\lambda+2\mu)\frac{\partial^2 v}{\partial y^2}+\mu\frac{\partial^2 v}{\partial x^2}+\mu\frac{\partial^2 v}{\partial z^2}+(\lambda+\mu)\frac{\partial^2 u}{\partial x\,\partial y}+(\lambda+\mu)\frac{\partial^2 w}{\partial y\,\partial z}=0 \tag{6b}$$

$$(\lambda+2\mu)\frac{\partial^2 w}{\partial z^2}+\mu\frac{\partial^2 w}{\partial x^2}+\mu\frac{\partial^2 w}{\partial y^2}+(\lambda+\mu)\frac{\partial^2 u}{\partial x\,\partial z}+(\lambda+\mu)\frac{\partial^2 v}{\partial y\,\partial z}=0 \tag{6c}$$

4 DERIVATION OF THE SOLUTIONS

In order to derive the solutions, it is assumed that the displacement functions u, v, and w may be represented using the following double trigonometric series in case of vertical loading. (*Note: due to lack of space, derivations for the case of horizontal loads in both x and y directions will not be presented in this paper*):

$$u=\sum_{m=1}^{\infty}\sum_{n=1}^{\infty}U(z)\sin(\xi_x x)\cos(\xi_y y) \tag{7a}$$

$$v=\sum_{m=1}^{\infty}\sum_{n=1}^{\infty}V(z)\cos(\xi_x x)\sin(\xi_y y) \tag{7b}$$

$$w=\sum_{m=1}^{\infty}\sum_{n=1}^{\infty}W(z)\cos(\xi_x x)\cos(\xi_y y) \tag{7c}$$

where, $U(z)$, $V(z)$, and $W(z)$ are the unknown displacement functions about the coordinate z and ξ_x and ξ_y are Fourier parameters for x and y coordinates, respectively. Substituting Eq 7 into Eq 6 and rearranging yields:

$$\mu\left(\frac{\partial^2}{\partial z^2}-\xi^2\right)U(z)-\xi_x(\lambda+\mu)\left(\frac{\partial W(z)}{\partial z}+\xi_x\,U(z)+\xi_y\,V(z)\right)=0 \tag{8a}$$

$$\mu\left(\frac{\partial^2}{\partial z^2}-\xi^2\right)V(z)-\xi_y(\lambda+\mu)\left(\frac{\partial W(z)}{\partial z}+\xi_x\,U(z)+\xi_y\,V(z)\right)=0 \tag{8b}$$

$$\mu\left(\frac{\partial^2}{\partial z^2}-\xi^2\right)W(z)+(\lambda+\mu)\left(\frac{\partial^2 W(z)}{\partial z^2}+\xi_x\,\frac{\partial U(z)}{\partial z}+\xi_y\,\frac{\partial V(z)}{\partial z}\right)=0 \tag{8c}$$

where $\xi^2=\xi_x^2+\xi_y^2$ and the solutions of $U(z)$, $V(z)$, and $W(z)$ are obtained as:

$$U(z)=C_3e^{\xi z}+C_4e^{-\xi z}+C_5\,e^{\xi z}z+C_6e^{\xi z}z \tag{9a}$$

$$V(z)=C_1e^{-\xi z}+C_2e^{\xi z}+\frac{C_3\,\xi_y\,e^{\xi z}}{\xi_x}+\frac{C_4\,\xi_y\,e^{-\xi z}}{\xi_x}+\frac{C_5\,\xi_y\,e^{\xi z}z}{\xi_x}+\frac{C_6\,\xi_y\,e^{-\xi z}z}{\xi_x} \tag{9b}$$

$$\begin{aligned}W(z)=&\frac{C_1\,\xi_y\,e^{-\xi z}}{\xi}-\frac{C_2\,\xi_y\,e^{\xi z}}{\xi}-\frac{C_3\,\xi e^{\xi z}}{\xi_x}+\frac{C_4\,\xi e^{-\xi z}}{\xi_x}+\\&C_5\left(-\xi z+\frac{(\lambda+3\mu)}{(\lambda+\mu)}\right)\frac{e^{\xi z}}{\xi_x}+C_6\left(\xi z+\frac{(\lambda+3\mu)}{(\lambda+\mu)}\right)\frac{e^{-\xi z}}{\xi_x}\end{aligned} \tag{9c}$$

Substituting Eq (9) in Eqs (2) and (4) and rearrange, the relationship between stresses and coefficients of integration is obtained to give transfer matrix for each layer as:

$$\begin{Bmatrix}U(z)\\V(z)\\W(z)\\\sigma_z(z)\\\tau_{zy}(z)\\\tau_{xz}(z)\end{Bmatrix}=\begin{bmatrix}t_{11}e^{-\xi z}&t_{12}e^{\xi z}&t_{13}e^{\xi z}&t_{14}e^{-\xi z}&t_{15}e^{\xi z}&t_{16}e^{-\xi z}\\t_{21}e^{-\xi z}&t_{22}e^{\xi z}&t_{23}e^{\xi z}&t_{24}e^{-\xi z}&t_{25}e^{\xi z}&t_{26}e^{-\xi z}\\t_{31}e^{-\xi z}&t_{32}e^{\xi z}&t_{33}e^{\xi z}&t_{34}e^{-\xi z}&t_{35}e^{\xi z}&t_{36}e^{-\xi z}\\t_{41}e^{-\xi z}&t_{42}e^{\xi z}&t_{43}e^{\xi z}&t_{44}e^{-\xi z}&t_{45}e^{\xi z}&t_{46}e^{-\xi z}\\t_{51}e^{-\xi z}&t_{52}e^{\xi z}&t_{53}e^{\xi z}&t_{54}e^{-\xi z}&T_{55}e^{\xi z}&t_{56}e^{-\xi z}\\t_{61}e^{-\xi z}&t_{62}e^{\xi z}&t_{63}e^{\xi z}&t_{64}e^{-\xi z}&t_{65}e^{\xi z}&t_{66}e^{-\xi z}\end{bmatrix}\begin{Bmatrix}C_1\\C_2\\C_3\\C_4\\C_5\\C_6\end{Bmatrix} \tag{10}$$

Coefficients of integration C_1, C_2, C_3, C_4, C_5 and C_6 are functions of ξ_x and ξ_y and are determined by using the known boundary conditions. After determining the coefficients of integration, Fourier inverse transform is performed on Eqs (10) to obtain displacements and stresses as shown below:

$$u=\frac{1}{2\pi}\int_{-\infty}^{\infty}\int_{-\infty}^{\infty}U(z)\sin(\xi_x x)\cos(\xi_y y)d\xi_x d\xi_y \tag{11a}$$

$$v = \frac{1}{2\pi}\int_{-\infty}^{\infty}\int_{-\infty}^{\infty} V(z)\cos(\xi_x x)\sin(\xi_y y)\, d\xi_x d\xi_y \tag{11b}$$

$$w = \frac{1}{2\pi}\int_{-\infty}^{\infty}\int_{-\infty}^{\infty} U(z)\cos(\xi_x x)\ \cos(\xi_y y) d\xi_x d\xi_y \tag{11c}$$

$$\sigma_{xx} = \frac{1}{2\pi}\int_{-\infty}^{\infty}\int_{-\infty}^{\infty} \sigma_{xx}(z)\cos(\xi_x x)\cos(\xi_y y) d\xi_x d\xi_y \tag{11d}$$

$$\sigma_{yy} = \frac{1}{2\pi}\int_{-\infty}^{\infty}\int_{-\infty}^{\infty} \sigma_{yy}(z)\cos(\xi_x x)\cos(\xi_y y) d\xi_x d\xi_y \tag{11e}$$

$$\sigma_{zz} = \frac{1}{2\pi}\int_{-\infty}^{\infty}\int_{-\infty}^{\infty} \sigma_{zz}(z)\cos(\xi_x x)\cos(\xi_y y) d\xi_x d\xi_y \tag{11f}$$

$$\tau_{xy} = \frac{1}{2\pi}\int_{-\infty}^{\infty}\int_{-\infty}^{\infty} \tau_{xy}(z)\sin(\xi_x x)\sin(\xi_y y) d\xi_x d\xi_y \tag{11g}$$

$$\tau_{xz} = \frac{1}{2\pi}\int_{-\infty}^{\infty}\int_{-\infty}^{\infty} \tau_{xz}(z)\cos(\xi_x x)\sin(\xi_y y) d\xi_x d\xi_y \tag{11h}$$

$$\tau_{yz} = \frac{1}{2\pi}\int_{-\infty}^{\infty}\int_{-\infty}^{\infty} \tau_{yz}(z)\cos(\xi_x x)\sin(\xi_y y) d\xi_x d\xi_y \tag{11i}$$

5 APPLICATION TO MULTILAYERED SYSTEM

Extension of the solutions to a multilayered system follows the procedure illustrated by Maina and Matsui (2004), which also utilizes transfer matrix. A multilayered system is as shown in Figure 2. Using layer matrix represented by Eq (10), the relation between responses on top and at the bottom of layer i may be given as follows:

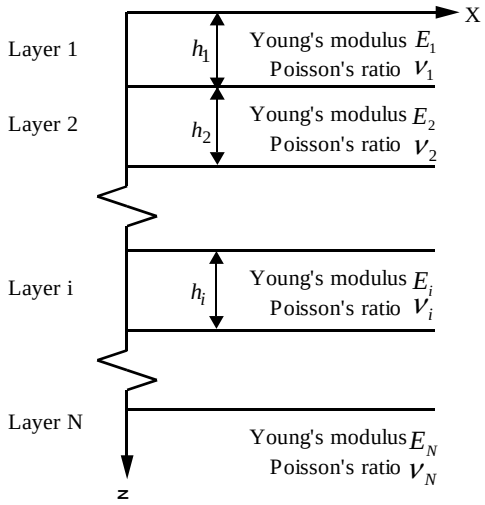

Figure 2: Model for multilayered elastic system

$$\begin{Bmatrix} U_{mn}^{(i)}(\xi_x,\xi_y,0) \\ V_{mn}^{(i)}(\xi_x,\xi_y,0) \\ W_{mn}^{(i)}(\xi_x,\xi_y,0) \\ \sigma_{z\,mn}^{(i)}(\xi_x,\xi_y,0) \\ \tau_{zy\,mn}^{(i)}(\xi_x,\xi_y,0) \\ \tau_{x\,z\,mn}^{(i)}(\xi_x,\xi_y,0) \end{Bmatrix} = \left[t_{jk}^{(1)}(\xi_x,\xi_y,0)\right]\left[t_{jk}^{(1)}(\xi_x,\xi_y,h_i)\right]^{-1} \begin{Bmatrix} U_{mn}^{(i)}(\xi_x,\xi_y,h_i) \\ V_{mn}^{(i)}(\xi_x,\xi_y,h_i) \\ W_{mn}^{(i)}(\xi_x,\xi_y,h_i) \\ \sigma_{z\,mn}^{(i)}(\xi_x,\xi_y,h_i) \\ \tau_{zy\,mn}^{(i)}(\xi_x,\xi_y,h_i) \\ \tau_{x\,z\,mn}^{(i)}(\xi_x,\xi_y,h_i) \end{Bmatrix} \tag{12}$$

where the superscript (i) in Eq (12) represents the layer number. The boundary condition at the interface of layers i and $i+1$ may be given as follows:

$$\begin{Bmatrix} U_{mn}^{(i)}(\xi_x,\xi_y,h_i) \\ V_{mn}^{(i)}(\xi_x,\xi_y,h_i) \\ W_{mn}^{(i)}(\xi_x,\xi_y,h_i) \\ \sigma_{z\,mn}^{(i)}(\xi_x,\xi_y,h_i) \\ \tau_{zy\,mn}^{(i)}(\xi_x,\xi_y,h_i) \\ \tau_{x\,z\,mn}^{(i)}(\xi_x,\xi_y,h_i) \end{Bmatrix} = \begin{Bmatrix} U_{mn}^{(i+1)}(\xi_x,\xi_y,0) \\ V_{mn}^{(i+1)}(\xi_x,\xi_y,0) \\ W_{mn}^{(i+1)}(\xi_x,\xi_y,0) \\ \sigma_{z\,mn}^{(i+1)}(\xi_x,\xi_y,0) \\ \tau_{zy\,mn}^{(i+1)}(\xi_x,\xi_y,0) \\ \tau_{x\,z\,mn}^{(i+1)}(\xi_x,\xi_y,0) \end{Bmatrix} \tag{13}$$

Using matrices from Eqs (12) and (13), the relationship between stresses and strains at the surface of layer 1 and coefficients of integration of layer N may be determined.

6 BOUNDARY CONDITION

Applying Fourier transform on the boundary condition defined by Eq (3) yields:

$$\sigma_k(\xi_x,\xi_y) = -p_k \frac{2\sin(a\xi_x)\sin(b\xi_y)}{\pi\,\xi_x\xi_y} \tag{14}$$

with $k = 1,2,3$ representing $\sigma_1 = \tau_{xz}(z)$, $\sigma_2 = \tau_{yz}(z)$, $\sigma_3 = \sigma_z(z)$, $p_1 = p_x$, $p_2 = p_y$, and $p_3 = p_z$, where $\sigma_z(z=0)$, $\tau_{xz}(z=0)$, and $\tau_{yz}(z=0)$ at the surface of layer 1 are known values. When $z \to \infty$ for the bottom layer N , all the responses will approach zero, which implies coefficients of integration $C_2^{(N)} = C_3^{(N)} = C_5^{(N)}$ will be zero. From the known surface conditions, unknown coefficients of integration $C_1^{(N)} = C_4^{(N)} = C_6^{(N)}$ may be determined.

7 EXTENSION TO MULTIPLE LOADING

Consider multiple loads shown in Figure 3. Analysis may be carried out by introducing a local coordinate system (x, y, z) whose origin is at the center of each load and the final responses may be determined by using the principle of superposition and referencing each load back to the global axis (X, Y, Z):

$$X = X_0 + x\,,\;\; Y = Y_0 + y\,,\;\; Z = Z_0 + z \tag{15}$$

where (X_0, Y_0, Z_0) is the distance of the origin of local coordinate system from the global coordinate system.

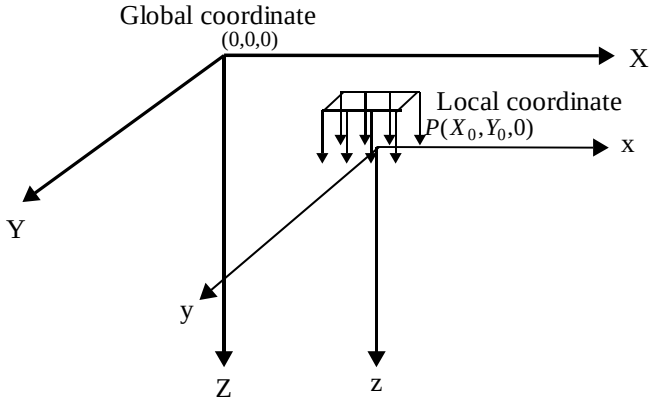

Figure 3: Global and local coordinate systems

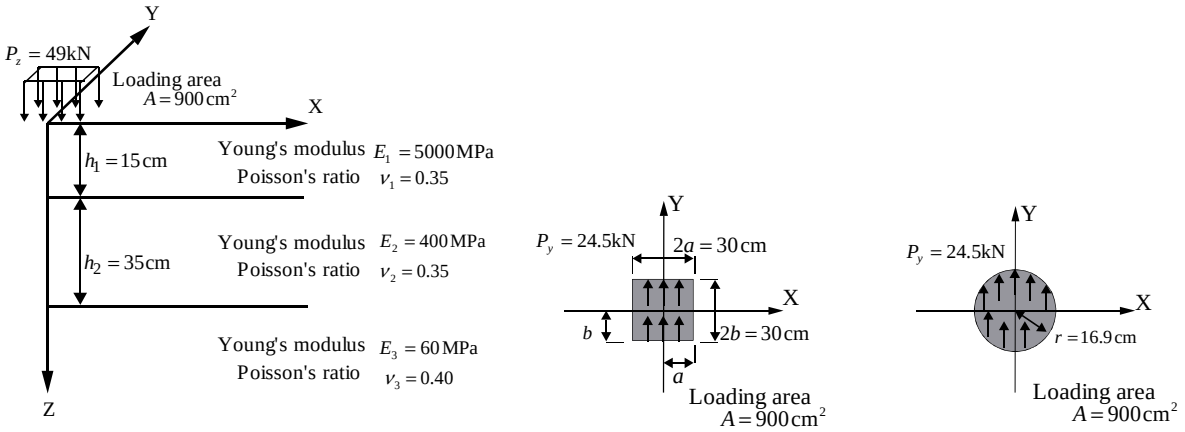

(a) Analytical model (b) Rectangular load (c) Circular load

Figure 4: Analytical model together with two load shapes

8. VALIDATION OF NUMERICAL ANALYSIS

In order to evaluate the viability of the algorithm developed, the 3-layered system shown in Figure 4 was analyzed considering two shapes of load. That is uniformly distributed rectangular and circular loads. The analysis of the rectangular load was performed using the theory described above and GAMES software was used to analyze the circular load (Maina and Matsui, 2004). Surface displacements and stresses within the multilayered system were compared. Furthermore, the calculated surface stress σ_z under rectangular load was compared with the boundary condition (external applied load) in order to confirm the accuracy of numerical analysis.

In this case, the center of the uniformly distributed load coincided with the center of the

global coordinate system $(X,Y)=(0,0)$. The magnitude of the load in the direction of Z-axis was $P_z=49\text{kN}$ and in the direction of Y-axis was $P_y=24.5\text{kN}$. The load shapes are shown in Figures 4(b) and 4(c), where the square load is $30\text{cm}\times30\text{cm}$ and for the area A of the circular load to be similar to the rectangular load with $A=900\text{cm}^2$, its radius was set to 16.9cm.

Results of surface displacement shown in Figure 5(a) were computed at $Z=0\text{cm}$, $X=0\text{cm}$ and $Y=0\sim150\text{cm}$. There is good match between results from circular and rectangular loads. Figure 5(b) shows results for σ_z and τ_{yz}, which were determined at $(X,Y)=(0,0)$ and $Z=0\sim150\text{cm}$. There is also good agreement of stresses, which validates the accuracy of the algorithm that was developed in this research.

The contour plot of surface stress is shown in Figure 5(c), which was produced by considering the symmetry of the load and utilized only the positive X, Y-axes. The theoretical boundary condition for σ_z within the loaded area ($X=Y<15\text{cm}$) was $\sigma_z=-5.44\text{MPa}$ and $\sigma_z=0\text{MPa}$ for $X=Y>15\text{cm}$, whereas at the edge of the load ($X=Y=15\text{cm}$) the stress, $\sigma_z=-2.72\text{MPa}$. Compared to the theoretical boundary condition values, Figure 6(c) shows some analytical errors in the vicinity ($X=Y=14\sim16\text{cm}$) of the load edge $X=Y=15\text{cm}$, while very good results were obtained elsewhere.

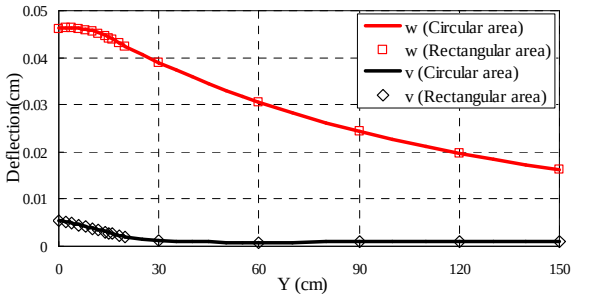

(a) Vertical displacement

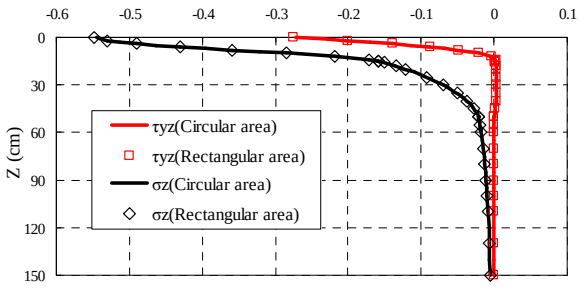

(b) Normal and shear stresses

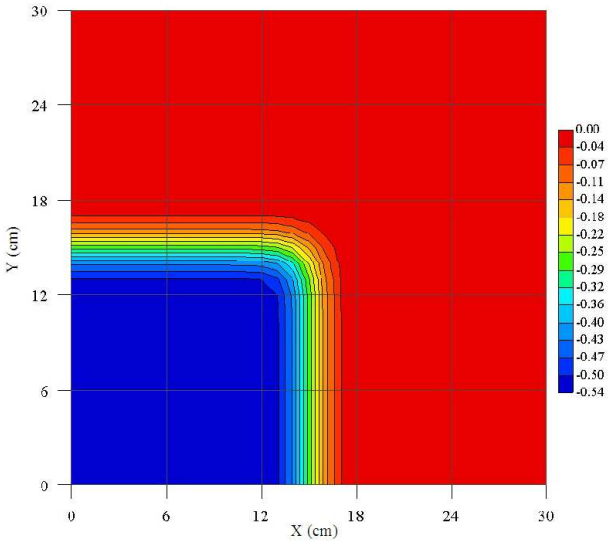

(c) Contour plot of surface stress

Figure 5: Analytical results

9 OBSERVATION AND CONCLUDING REMARKS

In this study, theoretical analysis of a multilayered system was successfully derived by using Cartesian coordinate system. It is important to point out that using this approach, uniform and

non-uniform rectangular loads may be analyzed.

From the worked examples presented, the following observations, mainly on primary responses, were made:

(1) Software, such as GAMES were developed for the purpose of determining pavement primary responses, at any point of interest, due to the action of uniformly distributed circular load. However, the method presented in this paper is capable of evaluating rectangular loads, which may not only be uniformly distributed but also non-uniformly distributed. Rectangular shaped load is used because it resembles tire footprints and the analysis will be more realistic.

(2) There was a very good overall match between responses due to uniform load over a rectangular area that was analyzed by the algorithm developed in this study and the uniformly distributed circular load that was analyzed using GAMES software.

(3) Although not presented in this paper, significant differences between circular and non-circular loads are anticipated when either multiple loads or non-uniform loads are analyzed.

ACKNOWLEDGMENT

This work was supported by Grant-in-Aid for Scientific Research (C) (20560435) in Japan and CSIR in South Africa.

REFERENCES

Borodachev, N. M., 1995. *Three-Dimensional Problem of the Theory of Elasticity in Strains*. Journal of Strength of Materials, Vol 27, No. 5-6.

Borodachev, N. M., 2001. *Construction of Exact Solutions to Three-Dimensional Elastic Problems in Stresses*. Journal of International Applied Mechanics, Vol 37, No. 6.

Borodachev, N. M. and Astanin, V. V., 2008. *Solution of a Three-Dimensional Problem of the Elasticity Theory in Terms of Displacements for an Isotropic Elastic Layer*. Journal of Strength of Materials, Vol 40, No. 3.

Bufler, H., 1971. *Theory of Elasticity of Multilayered Medium*. Journal of Elasticity, Vol. 1, No. 2, pp.125-143.

De Beer, M., 2008. *Stress-In-Motion (SIM) - A New Tool for Road Infrastructure Protection?*. International Conference on Heavy Vehicles (HVParis2008), Paris/Marne-la-Vallée.

Ernian, P., 1989. *Static response of a transversely isotropic and layered half-space to general surface loads.* Physics of the Earth and Planetary Interiors, 54, 353-363.

Maina, J. W. and Matsui, K., 2004. *Developing Software for Elastic Analysis of Pavement Structure Responses to Vertical and Horizontal Surface Loadings*. Transportation Research Records, No. 1896, pp. 107-118.

Morgan, G., Poulikakos, L., Arraigada. M, Muff, R., and Partl, M., 2008. *Stress-in-Motion Measurements of Heavy Vehicles from the Swiss Footprint Monitoring Site*. International Conference on Heavy Vehicles (HVParis2008), Paris/Marne-la-Vallée.

Ozawa, Y., Maina, J. W. and Matsui, K., 2009. *Linear Elastic Analysis of Pavement Structure Loaded over Rectangular Area*. 88th TRB Annual Meeting, Transportation Research Board, Washington D.C. USA. CD-ROM.

Ozawa, Y., Maina, J. W. and Matsui, K., 2010. *Analysis of Multilayered Half Space due to Rectangular Moving Load*. 89th TRB Annual Meeting, Transportation Research Board, Washington D.C. USA. CD-ROM.